

## COOPERATIVE LOCALIZATION-DELOCALIZATION IN THE HIGH $T_c$ CUPRATES

Julius RANNINGER

*Institut Néel, CNRS and Université Joseph Fourier, 25 rue des Martyrs, BP 166  
38042 Grenoble cedex 9, France\**

The intrinsic metastable crystal structure of the cuprates results in local dynamical lattice instabilities, strongly coupled to the density fluctuations of the charge carriers. They acquire in this way simultaneously both, delocalized and localized features. It is responsible for a partial fractioning of the Fermi surface, i.e., the Fermi surface gets hidden in a region around the anti-nodal points, because of the opening of a pseudogap in the normal state, arising from a partial charge localization. The high energy localized single-particle features are a result of a segregation of the homogeneous crystal structure into checker-board local nano-size structures, which breaks the local translational and rotational symmetry. The pairing in such a system is dynamical rather than static, whereby charge carriers get momentarily trapped into pairs in a deformable dynamically fluctuating ligand environment. We conclude that the intrinsically heterogeneous structure of the cuprates must play an important role in this type of superconductivity.

*Keywords:* Localization-delocalization; fermi surface fractioning; local symmetry breaking; crystalline metastability.

### 1. Introduction

The long standing efforts to synthesize superconductors with critical temperatures higher than about 25 K gradually faded away as the decades past. Three quarters of a century after the first discovery of superconductivity by Kamerlingh-Onnes<sup>1</sup> in 1911 (Hg with a  $T_c$  4.25 K), a ceramic material of not particularly good materials qualities surfaced in 1986 and Bednorz and Mueller produced this long searched after goal.<sup>2</sup> The inhomogeneities of these materials, which seem to be intrinsic, are related to local dynamical lattice instabilities, and could be a prime factor to bypass the limitation of  $T_c$ <sup>3</sup> in classical low temperature BCS type phonon-mediated superconductors.<sup>4</sup> Local dynamical lattice instabilities are known to trigger diamagnetic fluctuations<sup>5</sup> without leading to any global translational symmetry breaking, which would kill the superconducting state and end up in a charge ordered phase. Maximal values of  $T_c$  can be expected for materials, which are synthesized at the highest temperature in the miscibility phase diagram,<sup>6</sup> see Fig. 1. They present thermodynamically stable single-phase solutions at the boundary of insulating and metallic regions, which upon cooling condense into single-phase solid solutions.

---

\*julius.ranninger@grenoble.cnrs.fr

Their high kinetic stability prevents them from decomposing into the different compositions of the mixture one started with, due to a freezing-in of the high entropy mismatch of thermodynamically stable phases in the synthesis process. Microscopically, their metastability arises from adjacent cation-ligand complexes with incompatible inter-atomic distances.

Following such a strategy in material preparations,  $\text{BaBi}_x\text{Pb}_{1-x}\text{O}_3$ ,<sup>7</sup>  $\text{Ba}_{1-x}\text{K}_x\text{BiO}_3$ <sup>8,9</sup> and  $\text{Pb}_{1-x}\text{Tl}_x\text{Te}$ ,<sup>10,11</sup> just to mention a few representative examples, were synthesized and exhibited superconducting phases with  $T_c = 13, 30, 1.5$  K. These are relatively high values, considering their small carrier density of around  $10^{-20}/\text{cm}$ . Their parent compounds are respectively  $\text{BaBiO}_3$ , which is a diamagnetic insulating charge ordered state and  $\text{PbTe}$ , which is a small gap semiconductor. Their non-metallic phases are turned into superconductors upon partially substituting Bi by Pb, Ba by K and Te by Tl. According to band theory,  $\text{BaBiO}_3$  should be metallic, composed of exclusively  $\text{Bi}^{4+}$ . But the high polarizability of the oxygens<sup>12</sup> makes it synthesize in a mixture of  $\text{Bi}^{5+}$  and  $\text{Bi}^{3+}$ , rendering  $\text{Bi}^{4+}$  an unstable valence state. Such materials are sometimes referred to as “valence skippers”.  $\text{Bi}^{5+}$  occurs in a regular octahedral ligand environment, with a Bi–O distance of 2.12 Å.  $\text{Bi}^{3+}$ , on the contrary, occurs in a pseudo-octahedral ligand environment, with one of the oxygen ions in the octahedral being displaced to such an extent (with a corresponding Bi–O distance of 2.28 Å) that it effectively becomes  $\text{O}^{2-}$ , after having transferred an electron to  $\text{Bi}^{4+}$ .<sup>13</sup> This charge disproportionation results in negative U centers - the  $\text{Bi}^{3+}$  sites on which electrons pair up. The undoped parent compound stabilizes in a translational symmetry broken state of alternating  $\text{Bi}^{3+}$  and  $\text{Bi}^{5+}$  ions. Upon doping (partially replacing Bi by Pb), the system becomes superconducting with locally fluctuating  $[\text{Bi}^{3+} \leftrightarrow \text{Bi}^{5+}]$ , see Fig. 2. The situation is similar in  $\text{Pb}_{1-x}\text{Tl}_x\text{Te}$ . Its parent compound,  $\text{PbTe}$ , involves unstable  $\text{Te}^{2+}$  valence cations, which disproportionate into  $\text{Te}^{1+}$  and  $\text{Te}^{3+}$  ions, with the first again acting as negative U centers. Upon doping  $\text{PbTe} \rightarrow \text{Pb}_{1-x}\text{Tl}_x\text{Te}$  it changes into a superconductor, driven by those negative U centers.

## 2. The scenario

Cuprates High  $T_c$  materials bare some similarity to such so-called valence skipping compounds. Upon doping, their anti-ferromagnetic half-filled band Mott-insulating parent compound, composed of  $\text{Cu}^{II} - \text{O} - \text{Cu}^{II}$  bonds in the  $\text{CuO}_2$  planes, becomes dynamically locally unstable and leads to dynamically fluctuating  $\text{Cu}^{II} - \text{O} - \text{Cu}^{II} \leftrightarrow \text{Cu}^{III} - \text{O} - \text{Cu}^{III}$  bonds.<sup>14,15</sup> Different from the so-called valence skippers mentioned above, the basic building stones are covalent molecular bonds. This does not imply Cu valencies of 2+, respectively 3+. The notation II and III indicates stereochemical configurations defined by intrinsic Cu–O bond-lengths, which are 1.93 Å for  $\text{Cu}^{II} - \text{O} - \text{Cu}^{II}$  and 1.83 Å for  $\text{Cu}^{III} - \text{O} - \text{Cu}^{III}$ . Because of stereochemical misfits between the  $\text{CuO}_2$  planes and the surrounding cation-ligand complexes in the neighboring insulating planes, acting as charge reservoirs, the Cu - Cu dis-

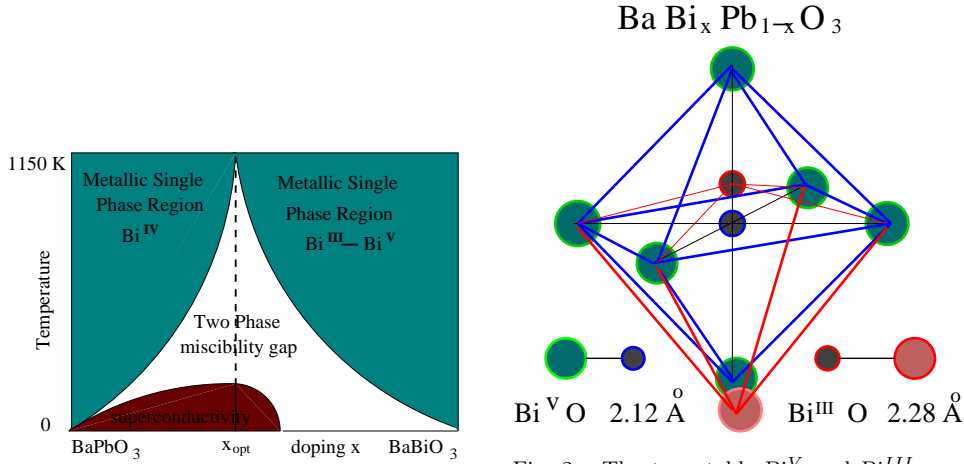


Fig. 1. Phasediagram for the  $\text{BaBi}_x\text{Pb}_{1-x}\text{O}_3$  synthesis (after Ref. 6).

Fig. 2. The two stable  $\text{Bi}^{\text{V}}$  and  $\text{Bi}^{\text{III}}$  configurations in regular and pseudo octahedral ligand environments (after Ref. 13).

tance of the  $\text{Cu}^{\text{II}} - \text{O} - \text{Cu}^{\text{II}}$  bonds in a square planar oxygen ligand environment are forced to reduce their lengths. They do that by a bond buckling, where the bridging oxygen of those bonds moves out of the  $\text{CuO}_2$  plane and thus respects its attributed stereochemical distance. Upon hole doping, the static bond buckling becomes dynamic, involving unbuckled linearly  $\text{Cu}^{\text{III}} - \text{O} - \text{Cu}^{\text{III}}$  bonds. The bridging oxygens then fluctuate in and out of the  $\text{CuO}_2$  plane and thus dynamically modulate the length of the  $\text{Cu} - \text{O}$  bonds. Experimentally, this feature is manifest in a splitting of the corresponding local bond stretch mode, which sets in in low doped metallic regime and disappears upon overdoping.<sup>16</sup> The two stereo-chemical configurations  $\text{Cu}^{\text{II}} - \text{O} - \text{Cu}^{\text{II}}$  and  $\text{Cu}^{\text{III}} - \text{O} - \text{Cu}^{\text{III}}$ , observed in EXAFS,<sup>17</sup> differ by two charges and it is that which results in the dynamically fluctuating diamagnetic bonds, which are the salient features of phase fluctuation driven superfluidity of the cuprates.<sup>18</sup> In spite of the huge differences in the  $\text{Cu} - \text{O}$  bond-length  $\simeq 0.1 \text{ \AA}$  of the  $\text{Cu} - \text{O} - \text{Cu}$  constituents, the cuprates do not break the overall translational symmetry caused by a charge order, but prefer to segregate into a local distribution of such bonds. They stabilize in a checkerboard structure of nano-size clusters, surrounded by small molecular  $\text{Cu}_4\text{O}_4$  sites, such that on a local basis those systems form a bipartite structure (see an idealized form for it in Fig. 3). The dynamically fluctuating uni-directional  $\text{Cu} - \text{O} - \text{Cu}$  bonds exist in two equivalent orthogonal directions and thus break not only the local translational but also rotational symmetry.<sup>19</sup> This prevents any tendency to long range translational symmetry breaking.

One might have expected such a result from the outset. Superconductivity in the cuprates is destroyed by phase fluctuations of the order parameter, without that its amplitude would suffer any significant depreciation.<sup>20,21</sup> This can only happen when Cooper pairs are fairly local entities, such as to provide superfluidity like features with a  $T_c$  scaling with the superfluid density at zero temperature<sup>18</sup> and XY

## 4 Julius RANNINGER

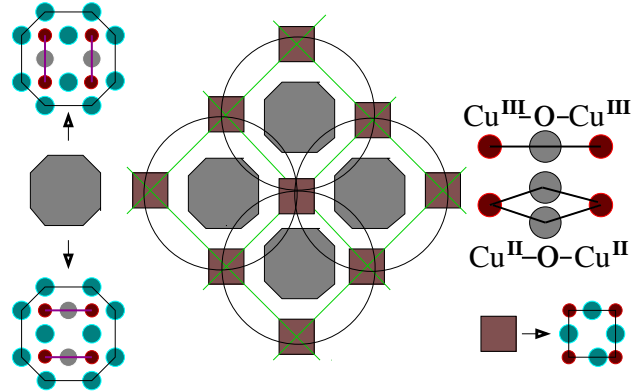


Fig. 3. Schematic view of the local segregation of the  $\text{CuO}_2$  planes into rotational symmetry breaking nano-size clusters (grey) (after Kohsaka *et al.* Ref. 19), containing dynamically deformable Cu-O-Cu bonds which act as pairing centers. These pairing centers are embedded in a metallic matrix of  $\text{Cu}_4\text{O}_4$  square (brown) plaquettes, on which the charge carriers circle around the central trapping centers, indicated by black circles. The small red filled circles indicate the Cu ions and the blue filled larger ones the oxygens. The fluctuating bridging oxygens are indicated by grey filled circles.

characteristics of the transition,<sup>22</sup> in strong contrast to the mean field characteristics of standard amplitude fluctuation controlled BCS superconductivity. The local nature of the Cooperons also implies that pairing correlations must develop already well above  $T_c$ . Because of the charged and local nature of the particles involved in this pairing, it has a strong effect on the local lattice deformations to which they are irrevocably coupled.

In principle one can now envisage two scenarios:

(i) if the coupling is very strong, the charge carriers form bipolarons, which in principle can condense into a superfluid phase - the Bipolaronic Superfluidity,<sup>23</sup> but which are more likely to end up in an insulating state of statically disordered localized bipolarons, if not a charge ordered state of them.<sup>24</sup>

(ii) if the coupling is not quite as strong, the charge carriers will be in a mixture of quasi-free itinerant states and localized states, where they are momentarily self-trapped in form of local bound pairs. Local dynamical pairing then occurs at some temperature  $T^*$ , at which the single-particle density of states develops a pseudogap, because of the electrons getting paired up on a finite time scale.<sup>25</sup> Upon lowering the temperature, those phase incoherent locally dynamically fluctuating pairs acquire short range phase coherence, which ultimately leads to their condensation and phase locking in a superfluid state at some temperature  $T_\phi$ , exclusively controlled by phase fluctuations.<sup>26</sup> Experimental evidence for that is now well established in terms of the transient Meissner effect,<sup>27</sup> the Nernst effect in thermal transport,<sup>28</sup> the torque measurements of diamagnetism<sup>29</sup> and a proximity induced pseudogap of metallic films deposited on  $\text{La}_{2-x}\text{Sr}_x\text{CuO}_4$ .<sup>30</sup>

Standard low temperature BCS superconductors are controlled by amplitude fluctuations, with the feature that at  $T_c$  the expectation value of the amplitude vanishes, i.e., the number of Cooper pairs goes to zero and thus the phase of the order parameter becomes redundant. For superfluid He, the opposite is the case. The onset of superfluidity is controlled exclusively by spatial phase locking of the bosonic order parameter. The amplitude there is fixed, since the number of bosonic He atoms is conserved. The superfluid state is destroyed at a certain  $T_\phi$ , given by the phase stiffness of the condensate. The high  $T_c$  superconductors lie between those two limiting cases. Amplitude and phase fluctuations are then strongly inter-related and have to be treated on equal footing. The onset of a finite amplitude of the order parameter happens at a temperature  $T^*$ , while that of the phase locking of the bosonic Cooperons, signaling the onset of superconductivity, occurs at  $T_\phi$ , which can be well below  $T^*$ . Dealing with such a situation requires to disentangle the description of phase and amplitude fluctuations of the Cooperons. Cooperons are neither true bosons nor hard-core bosons, but their center of mass can be associated to bosons in real space. Using a renormalization procedure one can project out such bosons of the Cooperons, leaving us with remnants arising from kinematical interactions due to their non-bosonic statistics coming from their internal fermionic degrees of freedom. That leads to a damping of such bosons. Those bosons have an amplitude and a phase and hence can account for both: (i) their dissociation into fermion pairs at  $T^*$ , where their amplitude disappears together with the closing of the pseudogap in the fermionic single-particle subsector and (ii) the breaking up their spatial phase coherence at  $T_\phi$ , where the bosons enter into a phase disordered boson metallic state, albeit keeping short range phase coherence in a finite temperature regime above  $T_\phi$ . This scenario follows some old ideas in the early days of the BCS theory, when exploring the interaction between the electrons and the Cooper pairs in a perturbative way,<sup>31</sup> or, in a more recent study, using a phenomenological picture for strong inter-relations between the two.<sup>32</sup> In the approach we have been following now for several years, the inter-relation between phase and amplitude fluctuations is cast into Andreev scattering of the fermions on bosons. It results in a partial trapping of the fermions in form of localized bound fermion pairs in real space, and leads to fermionic excitations, which are in a superposition of itinerant and localized states, consistent with recent STM imaging results.<sup>19</sup> The pairing we are considering here corresponds to a resonant pairing, induced by fluctuating molecular bonds driven by intrinsic dynamical lattice instabilities. The mechanism is similar to that of a Feshbach resonance<sup>33</sup> in fermionic atom gases, where fermionic atoms exist simultaneously in form of scattering electron-spin singlet states and as bound electron-spin triplet states.

### 3. The model

Resonant pairing systems can most efficiently be described by a Boson Fermion Model (BFM), such as I had conjectured shortly after the proposition of the Bipolaron

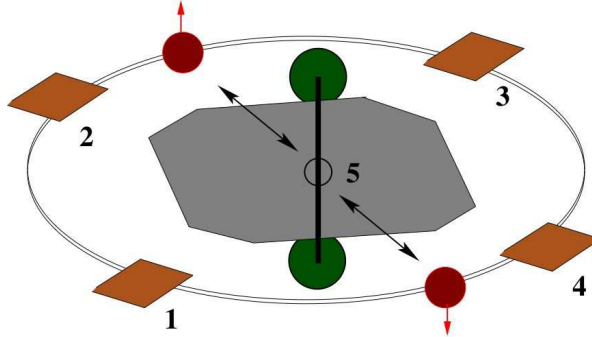
6 *Julius RANNINGER*

Fig. 4. Simplified version of a local cluster of Fig. 3, composed of (i) a trapping domain  $\text{Cu}_4\text{O}_{10}$ , replaced here by a deformable dumbbell oscillator (green filled circles) at site 5, capable of trapping two electrons (red filled circles) in form of a bipolaron and (ii) four  $\text{Cu}_4\text{O}_4$  square plaquettes, which are replaced by effective sites 1 - 4, on which the electrons circle around the central site 5.

laronic Superconductivity.<sup>23</sup> This phenomenological model represents a mixture of itinerant fermions and localized bosons —locally bound fermion pairs— with an exchange interaction between the two. A common chemical potential is assumed such as to assure that we are dealing with a unique species of charge carriers. They must exist simultaneously in (i) itinerant states circling around the trapping centers and (ii) as localized states on the trapping centers, the moment they pair up. This picture is quite general and does not depend on any specific mechanism for pairing. It can arise from holes in a strongly correlated Hubbard system close to half filling,<sup>34</sup> where the exchange happens between hole singlet-pairs and itinerant uncorrelated holes<sup>35</sup> or, as we have been pursuing it for years, from a polaronic mechanism.

Our picture of hole-doped cuprates is based on an ensemble of effective sites, embedded in a crystalline structure, each one being composed of a deformable cation-ligand complex, surrounded by an undeformable local environment, the four-site rings, see Fig. 3. The local environments of neighboring deformable molecular clusters overlap with each other, which assures a potentially metallic phase of the charge carriers. If the coupling of electrons into bosonic bound pairs outweighs their kinetic energy, it leads to a Bose liquid, which can be either superfluid or insulating, without that any fermions are present in the background. High  $T_c$  materials do however exhibit such a background Fermi sea and at the same time a transition into a superfluid state which is governed by the dynamics of bosonic fermion-pairs rather than by the opening up of a gap in the electronic single-particle density of states. Itinerant bosons are induced upon hole doping. They form and disappear spontaneously on the deformable cation-ligand clusters and thereby break the crystal symmetry on a local level. This resonating pairing originates from the local dynamical lattice instabilities and metastability of the cuprates. It implies that those systems are intrinsically inhomogeneous, having segregated, upon doping, into effective sites of molecular clusters, partially occupied by such bosons. Resonating pairs of fermions,

implies electrons fluctuating in and out of those deformable clusters, on which they self-trap themselves in form of bound pairs on a finite time scale. This situation is energetically more favorable than that of purely localized bosonic bound fermion pairs or itinerant uncorrelated fermions. It benefits from a lowering of the ionic level due to a polaron level shift and from the bound fermion pairs acquiring itinerancy.

Let us now demonstrate that on the basis of a small cluster calculations, following a previous detailed study<sup>37</sup> on that. The segregation of the  $\text{CuO}_2$  plane charge distribution, upon hole doping, has been seen in STM imaging studies<sup>19</sup> and a sketch for such segregation is illustrated in Fig. 3. It consists of nano-size  $\text{Cu}_4\text{O}_{10}$  domains composed of deformable Cu - O - Cu bonds which are capable of trapping momentarily two itinerant holes from the surrounding  $\text{Cu}_4\text{O}_4$  plaquettes. Those latter form the remnant back bone structure corresponding to the undoped cuprates carrying the itinerant charge carriers. The fluctuation of the charge carriers back and forth between the two subcomponents of the segregated  $\text{CuO}_2$  planes ultimately induces a diamagnetic component among the itinerant charge carriers.

#### 4. Resonant pairing and local dynamical lattice instabilities

The physics elaborated above is an intrinsic property of the nano-size  $\text{Cu}_4\text{O}_{10}$  clusters, making up those materials. We illustrate that by mapping the central  $\text{Cu}_4\text{O}_{10}$  trapping domain together with its four surrounding  $\text{Cu}_4\text{O}_4$  plaquettes, into a tractable model: a central effective site given by a deformable oscillator surrounded by four atomic sites (see Fig. 4). On the first, the itinerant charge carriers can get self trapped into localized bipolarons, corresponding to a deformation which mimics the process  $\text{Cu}^{III} - \text{O} - \text{Cu}^{III} \Leftrightarrow \text{Cu}^{II} - \text{O} - \text{Cu}^{II}$  in the trapping domains of Fig. 3. Resonant pairing occurs when the energies of the bipolaronic level corresponds to the Fermi energy of the itinerant fermionic subsystem. In our toy model we shall characterize these states by two-electron eigenstates on the four-site ring. The Hamiltonian for such a small cluster system is given by

$$\begin{aligned}
 H = & -t \sum_{i \neq j=1 \dots 4, \sigma} \left[ c_{i,\sigma}^\dagger c_{j,\sigma} + h.c. \right] - t^* \sum_{i=1 \dots 4, \sigma} \left[ c_{i,\sigma}^\dagger c_{5,\sigma} + h.c. \right] \\
 & + \Delta \sum_{\sigma} c_{5,\sigma}^\dagger c_{5,\sigma} + \hbar\omega_0 \left[ a^\dagger a + \frac{1}{2} \right] - \hbar\omega_0 \alpha \sum_{\sigma} c_{5,\sigma}^\dagger c_{5,\sigma} [a + a^\dagger], \quad (1)
 \end{aligned}$$

where  $c_{i\sigma}^{(\dagger)}$  denotes the annihilation (creation) operator for an electron with spin  $\sigma$  on site  $i$ , and  $a_5^{(\dagger)}$  the phonon annihilation (creation) operator associated with a deformable cation-ligand complex at site 5.  $\alpha$  denotes the dimensionless electron-phonon coupling constant,  $\omega_0$  the Einstein oscillator frequency of the local dynamical deformation on the central polaronic site 5,  $t$  the intra-ring hopping integral and  $t^*$  the one controlling the transfer between the ring and the central site 5.  $\Delta$  denotes the bare energy of the electrons when sitting on site 5. before they couple to the local lattice deformation. This local cluster describes the competition between

8 *Julius RANNINGER*

localized bipolaronic electron pairs on the central cation-ligand complex and itinerant electrons on the plaquette sites, when the energies of the two configurations are comparable with each other, i.e. for  $2\Delta - 4\hbar\omega_0\alpha^2 \simeq -4t$ . There is a narrow resonance regime where this happens, as we can see from the strong enhancement of the efficiency rate  $F_{\text{exch}}^{\text{pair}}$

$$F_{\text{exch}}^{\text{pair}} = \langle GS | c_{5,\uparrow}^\dagger c_{5,\downarrow}^\dagger c_{q=0,\downarrow} c_{q=0,\uparrow} | GS \rangle - \langle GS | c_{q=0,\uparrow}^\dagger c_{5,\uparrow}^\dagger | GS \rangle \langle GS | c_{q=0,\downarrow}^\dagger c_{5,\downarrow} | GS \rangle \quad (2)$$

for transferring electron pairs back and forth between the ring sites and the central polaronic site,<sup>9</sup> (see Fig. 5) and where we have subtracted out the exchange due to incoherent single-electron processes.  $|GS\rangle$  denotes the ground state of the cluster. This resonant scattering process induces a diamagnetic component of the electrons moving on the ring. The density  $n_p$  of such diamagnetically correlated resonantly induced pairs is given by

$$n_p = \langle n_{q=0,\uparrow} n_{q=0,\downarrow} \rangle - \langle n_{q=0,\uparrow} \rangle \langle n_{q=0,\downarrow} \rangle \quad (3)$$

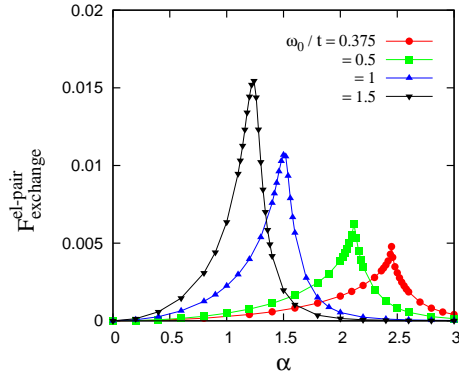


Fig. 5. (Color online) The efficiency factor  $F_{\text{exch}}^{\text{pair}}$  as a function of  $\alpha$  for converting a localized bipolaron on the central polaronic complex into a pair of diamagnetically correlated electrons on the ring, for several adiabaticity ratios  $\omega_0/t$  (after Ref. 37).

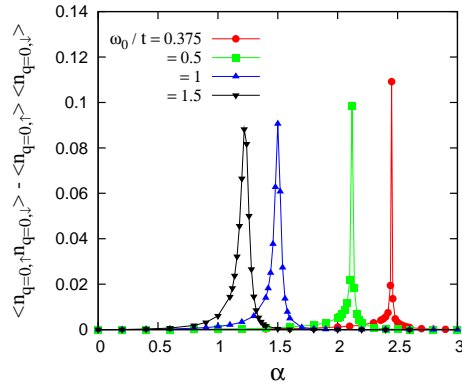


Fig. 6. (Color online) Density  $n_p$  of diamagnetically correlated electron pairs on the ring as a function of  $\alpha$  showing a strong enhancements for  $\alpha = \alpha_c$  for a set of adiabaticity ratios  $\omega_0/t$  (after Ref. 37).

The variation of  $n_p$  with  $\alpha$  (Fig. 6) shows an equally sharp enhancement near the resonance  $\alpha_c$ , which depends on the adiabaticity ratio  $\omega_0/t$ . Its relative density is quite sizable - about 20% of the total average density of electrons on the ring at  $\alpha_c$ . Slightly away from this resonant regime, the electrons are either pair-uncorrelated (for  $\alpha \leq \alpha_c$ ) or not existent on the plaquette (for  $\alpha \geq \alpha_c$ ), because of being confined to the polaronic cation-ligand complex as localized bipolarons.

The features driving these electronic exchange are local deformations of the molecular dimer, which induce a correlated dynamics of the local dimer deformations

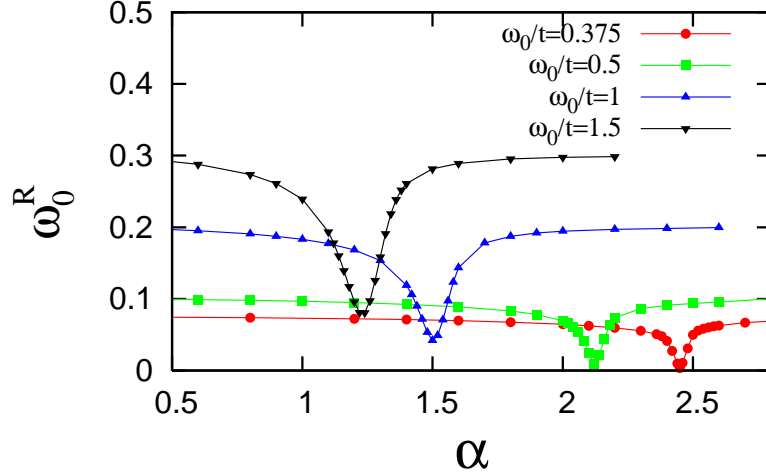


Fig. 7. (Color online) The phonon softening as a function of the electron-dimer coupling constant for various adiabaticity ratios  $\omega_0/t = 0.375, 0.5, 1$  and  $1.5$  (after Ref. 37).

and the local charge fluctuations. Denoting the modulation in length of the dimer by  $X = \sqrt{\hbar/2M\omega_0}[a^+ + a]$ , the corresponding phonon Greens function is

$$D_{ph} = \frac{2M\omega_0}{\hbar} \langle\langle X; X \rangle\rangle, \quad (4)$$

where  $M$  denotes the mass of the vibrating dimer atoms (green in Fig. 4). Our previous results<sup>37</sup> on this local lattice dynamics are reproduced in Fig. 7, where we illustrate the softening of the bare phonon mode  $\omega_0$  down to  $\omega_0^R$  at the resonance. It is this frequency which determines the correlated charge-deformation fluctuations and provides us with an estimate for the effective mass of the diamagnetic pairs (see the discussion in the SUMMARY section of Ref. 37).

## 5. Separation of phase and amplitude variables

Molecular clusters, like the one discussed in the previous section, form the building blocks of hole doped segregated  $\text{CuO}_2$  planes and which, accordingly assembled, form the macroscopic cuprate structure: a regular bipartite lattice structure, idealized in Fig. 3. This picture is in accordance with the checker-board structure seen in STM imaging studies.<sup>19</sup> The local stability of such dynamically fluctuating molecular clusters is obtained at resonance, i.e., at  $\alpha_c$ , which depends on the adiabaticity ratio but more sensibly on the exchange rate  $\propto \omega_0^R$  between the localized pairs and the itinerant electrons. This latter will strongly depend on the degree of hole doping.

The microscopic mechanism for hole doping in the cuprates is a complex phenomenon and far from being understood. The undoped systems present a homogeneous lattice structure with buckled  $\text{Cu}^{II} - \text{O} - \text{Cu}^{II}$  molecular bonds. Due to strong Hubbard correlations among the electrons in such a half-filled band system,

the ground state is an antiferromagnetic insulator. Upon slight hole doping it breaks down into a glassy heterogeneous structure, which we interpret in our scenario as a phase uncorrelated bipolaronic Mott insulator,<sup>26,38</sup> composed of  $\text{Cu}^{II} - \text{O} - \text{Cu}^{II}$  covalent molecular bonds, behaving as hardcore intersite bipolarons. Upon increasing the hole doping beyond around 0.10 per Cu ion, the system segregates into a checkerboard structure with nano-size molecular Cu - O - Cu clusters, in a mixture of  $\text{Cu}^{II} - \text{O} - \text{Cu}^{II}$  and  $\text{Cu}^{III} - \text{O} - \text{Cu}^{III}$  molecular bonds. These nano-size clusters act as trapping centers for the itinerant electrons moving on the sublattice in which those cluster are embedded (see Fig. 3). Given the experimental findings on the effect of hole doping on the crystal structure monitored by an increase in covalency,<sup>39</sup> we conjecture that hole doping primarily induces hole-bipolarons ( $\text{Cu}^{III} - \text{O} - \text{Cu}^{III}$  molecular bonds) on the nano-size trapping centers. This triggers local charge fluctuations, by momentarily capturing two electrons from of the surrounding four-site ring environment, transforming  $\text{Cu}^{III} - \text{O} - \text{Cu}^{III}$  into  $\text{Cu}^{II} - \text{O} - \text{Cu}^{II}$  molecular bonds. The two initially uncorrelated electrons thereby acquire a diamagnetic component, which they keep upon returning into the itinerant subsystem via the inverse process  $[\text{Cu}^{II} - \text{O} - \text{Cu}^{II}] \rightarrow [\text{Cu}^{III} - \text{O} - \text{Cu}^{III}]$ .

This resonant back and forth scattering between bound and unbound electrons stabilizes the dynamical transfer of a small fraction of electrons  $n_F^h$  from the initially quasi half-filled band of itinerant charge carriers into the trapping centers. As a result, the Fermi surface shrinks, which implies a hole density  $n_F^h = n_B$  of single-particle excitations. Since  $n_F^h$  varies only in a small regime, between 0.10 and 0.22, covering the superconducting phase, we choose for our resonant pairing scenario, a total number of charge carriers around  $n_{\text{tot}} = n_F + n_B \simeq 1$ , which will slightly decrease with hole doping. This will lead to a self-regulating boson density, such as  $n_B \leq 0.08$  for the optimally doped case  $n_F^h \simeq 0.16$ . The electrons, being momentarily trapped into bound electron pairs on the deformable molecular clusters, can be associated to bosonic variables  $b^{(\dagger)}$  with  $n_B = \langle b^\dagger b \rangle$ . Our further analysis is based on the BFM which, in momentum space, is given by the Hamiltonian

$$H_{\text{BFM}} = H_{\text{BFM}}^0 + H_{\text{BFM}}^{\text{exch}} \quad (5)$$

$$H_{\text{BFM}}^0 = \sum_{\mathbf{k}\sigma} (\varepsilon_{\mathbf{k}} - \mu) c_{\mathbf{k}\sigma}^\dagger c_{\mathbf{k}\sigma} + \sum_{\mathbf{q}} (E_{\mathbf{q}} - 2\mu) b_{\mathbf{q}}^\dagger b_{\mathbf{q}}. \quad (6)$$

$$H_{\text{BFM}}^{\text{exch}} = (1/\sqrt{N}) \sum_{\mathbf{k}, \mathbf{q}} (g_{\mathbf{k}, \mathbf{q}} b_{\mathbf{q}}^\dagger c_{\mathbf{q}-\mathbf{k}, \downarrow} c_{\mathbf{k}, \uparrow} + H.c.) \quad (7)$$

$$H_{\text{BFM}}^{F-F} = \frac{1}{N} \sum_{\mathbf{p}, \mathbf{k}, \mathbf{q}} U_{\mathbf{p}, \mathbf{k}, \mathbf{q}} c_{\mathbf{p}\uparrow}^\dagger c_{\mathbf{k}\downarrow}^\dagger c_{\mathbf{q}\downarrow} c_{\mathbf{p}+\mathbf{k}-\mathbf{q}\uparrow}. \quad (8)$$

Following the basic electronic structure of the cuprates, we assume a d-wave symmetry for the boson-fermion exchange interaction  $g_{\mathbf{k}, \mathbf{q}} = g[\cos k_x - \cos k_y]$ , between (i) pairs of itinerant charge carriers  $c_{\mathbf{k}\sigma}^{(\dagger)}$  circling around the polaronic sites and (ii) the polaronically bound pairs of them  $b_{\mathbf{q}}^{(\dagger)}$ , when these same charge

carriers have hopped onto this site and got self trapped. The anisotropy of the itinerant charge carrier dispersion is assured by the standard expression  $\varepsilon_{\mathbf{k}} = -2t[\cos k_x + \cos k_y] + 4t' \cos k_x \cos k_y$  for the  $\text{CuO}_2$  planes with  $t'/t = 0.4$ . The strength of the boson-fermion exchange coupling in our effective Hamiltonian can be estimated from our study of the single cluster problem and is given by  $F_{\text{exch}}^{\text{pair}}$ , which is related to the electron-lattice coupling  $\alpha$  and the bare phonon frequency  $\omega_0$ , as discussed in detail in Ref. 37. In order to get an insight into the inter-related amplitude and phase fluctuations in hole doped High  $T_c$  cuprates, we transform this Hamiltonian by a succession of unitary transformations into a block diagonal form, composed of exclusively (i) renormalized fermionic particles and (ii) renormalized bosonic particles. This gives us an access to study the characteristic single-particle spectral properties such as the pseudogap and the two-particle-properties, controlling the onset of phase locking and diamagnetic fluctuations, which govern the transport as one approaches  $T_c$  from above. Using Wegner's Flow Equation renormalization procedure<sup>36</sup> we eliminate the boson-fermion exchange coupling in successive steps, obtaining a Hamiltonian of the same structure as the initial one, Eqs (5–8), but with renormalized parameters  $g^* = 0$ ,  $\varepsilon_{\mathbf{k}}^*$ ,  $E_{\mathbf{q}}^*$ ,  $U_{\mathbf{p},\mathbf{k},\mathbf{q}}^*$ , which have evolved out of the bare ones we started with, i.e.,  $g, \varepsilon_{\mathbf{k}}, E_{\mathbf{q}} = \Delta - \mu, U_{\mathbf{p},\mathbf{k},\mathbf{q}} = 0$ . The chemical potential  $\mu$ , which also evolves in the course of this renormalization procedure is determined at each step of it, such as to assure a given total density of fermionic and bosonic particles  $n_{\text{tot}}$ . From our detailed calculations<sup>40</sup> of this renormalized Hamiltonian and its spectral properties we see a transformation of the electron dispersion, close to the chemical potential, which changes into an S-like shape upon lowering the temperature below a certain  $T^*$ . It signals the onset of pairing and manifests itself in a corresponding opening of the pseudogap in the single-particle density of states. Simultaneously the intrinsically dispersion-less bosons acquire a  $q^2$  like spectrum, albeit overdamped until, upon further decreasing the temperature, they finish up as well defined quasi-particle which ultimately condense into a superfluid phase below  $T = T_\phi$ . Their  $q^2$  like spectrum transforms into a linear in  $q$  branch, which signals the phase locked superfluid state of those bosons.

The anisotropic d-wave structure of the boson-fermion exchange coupling implies a variation of its strength, going from zero at the nodal points  $[\pm\pi/2, \pm\pi/2]$  of the Fermi surface toward its maximal value, equal to  $g$ , near the hotspots  $\mathbf{k} = [0, \pm\pi]$ ,  $[\pm\pi, 0]$ . Upon moving on an arc in the Brillouin zone, corresponding to the chemical potential, i.e.,  $\varepsilon^*(k_x, k_y) = \mu$ , one observes a well defined Fermi surface around the nodal points. But upon parting from this limited region, the Fermi surface gets hidden because of the onset of a pseudogap. This has been called "Fermi Surface Fractionation". It implies in this region of the Brillouin zone (see Fig. 8) three astonishingly related features: (i) diffusively propagating Bogoliubov branches below  $\omega = 0$  for  $\mathbf{k} \geq \mathbf{k}_F$ , indicated by  $A_{inc}^F(\mathbf{k}, \omega)$  (black lines). They are remnants of superconducting phase locking on a finite space-time scale, which have been predicted by us in 2003<sup>41</sup> and only very recently have been verified by ARPES in

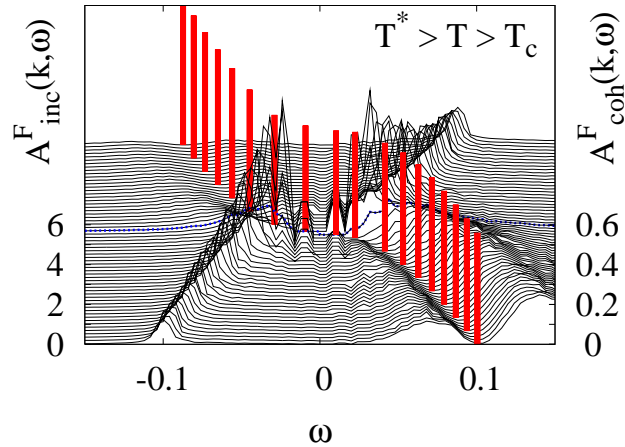


Fig. 8. The single-particle spectral function  $A(\mathbf{k}, \omega) = A_{\text{inc}}(\mathbf{k}, \omega) + A_{\text{coh}}(\mathbf{k}, \omega)$  in the pseudogap phase around the hidden “Fermi surface” ( $\omega = 0$ ) and near the anti-nodal point. The set of curves corresponds to different  $\mathbf{k}$  vectors, orthogonally intersecting the hidden Fermi surface. The curve in blue indicates the spectrum exactly at this hidden Fermi surface (after Ref. 40).

2008,<sup>42</sup>; (ii) localized high energy modes above  $\omega = 0$  (black) for  $\mathbf{k} \geq \mathbf{k}_F$ , which occur together with those diffusively propagating Bogoliubov modes. We have interpreted them as the internal degrees of freedom of those two-particle collective phase modes, showing up in their high frequency response. They present locally partially trapped single-particle states making up the bipolaronic Cooperons,<sup>40</sup> which include; (iii) in-gap single-particle contributions, denoted by  $A_{\text{coh}}^F(\mathbf{k}, \omega)$  (red delta like peaks). Their weight should be understood as the overall spectral weight for very broadened peaks, as we know from independent studies, such as self-consistent perturbative treatments<sup>25</sup> and DMFT procedures.<sup>43</sup> The characteristic three-peak structure of the single-particle spectral features for  $\mathbf{k} \geq \mathbf{k}_F$  in this part of the Brillouin zone around the hidden Fermi surface is a fingerprint of resonant pairing systems, highlighting their deviations from BCS like superconductivity, for which the spectral features would invariably provide a two peak structure. The recent STM imaging studies are further proof of the non-BCS like features of the spectral properties attributed to in-gap single-particle contributions above  $T_c$ .

## 6. Summary

Exploiting the intrinsic metastability of hole doped cuprates, we investigated a scenario of resonant pairing, driven by dynamical local lattice instabilities. It invokes charge carriers, which simultaneously exist as itinerant quasi-particles and as localized self-trapped bipolarons. The quantum fluctuations between the two configurations induce mutually (i) a certain degree of itinerancy of the bare localized

bipolarons and (ii) localized features in the single-particle spectral function. This is evident in simultaneously featuring a low energy diffusive Bogoliubov branch below the chemical potential and single-particle excitations, accompanied by remnant bonding and anti-bonding states in the high energy response, above the chemical potential. These are finger prints of the non-BCS like physics of those cuprates, which should be interesting to test experimentally and link up with studies of anomalous lattice properties which are at the origin of the dynamical lattice instability driven segregation of the homogeneous cuprate lattice structure into checker-board structures.

### Acknowledgements

I would like to thank my colleagues Tadek Domanski and Alfonso Romano for having participated in numerous theoretical studies on which this present attempt, to develop a global picture of the cuprates, is based. I thank Juergen Roehler, who kept me regularly informed about relevant experimental results as well and his critical and constructive comments, which helped me in my understanding those materials.

### References

1. H. Kamerlingh-Onnes, Leiden Comm. 120 b (1911).
2. J. G. Bednorz and K. A. Mueller, Z. Phys. B-Condensed Matter **64**, 189 (1986).
3. P. W. Anderson and B. T. Matthias, Science **144**, 373 (1964).
4. J. Bardeen, L. N. Cooper and J. R. Schrieffer, Phys. Rev, **108**, 1175 (1957).
5. J. M. Vandenberg and B. T. Matthias, Science **198**, 194 (1977).
6. A. W. Sleight, Physics Today, **44**(6), 24 (1991).
7. A. W. Sleight, J. L. Gillson and P. E. Bierstedt, Solid State Commun. **17**, 27 (1975)-
8. R. J. Cava et al., Nature (London) **332**, 814 (1988).
9. D. G. Hinks et al., Nature (London) **333**, 836 (1988).
10. I. A. Chernik and S Lykov Sov. Phys. Solid State **23**, 1724 (1981).
11. B. Ya. Moizhes and I. Drabkin Sov. Phys. Solid State **25**, 1139 (1983).
12. I. Hase and T. Yanagisawa, Phys. Rev. B **76**, 174103 (2007).
13. A. Simon, Chem. Unserer Zeit **22**, 1 (1988).
14. Y. Kohsaka et al., Science **315**, 1380 (2007).
15. K. K. Gomes et al., Nature **447**, (2007).
16. D. Reznik et al., Nature **440**, 1170 (2006).
17. C. J. Zhang and H. Oyanagi, Phys. Rev. B **79**, 064521 (2009).
18. Y. J. Uemura et al., Phys. Rev. Lett., **62**, 2317 (1989).
19. Y. Kohsaka et al., Nature **454**, 1072 (2008).
20. V. J. Emery and S. A. Kivelson, Nature, **374**, 434 (1995).
21. M. Franz and A. J. Millis, Phys. Rev. B **58**, 14572 (1998).
22. M. B. Salamon et al., Phys. Rev. B **47**, 5520 (1993).
23. A. S. Alexandrov and J. Ranninger, Phys. Rev. B **23**, 1796 (1981) and Phys. Rev. B **24**, 1164 (1981).
24. B. K. Chakraverty, J. Ranninger and D. Feinberg, Phys. Rev. Lett., **81**, 433 (1998).
25. J. Ranninger, J.M. Robin, and M. Eschrig, Phys. Rev. Lett. **74**, 4027 (1995).
26. M. Cuoco and J. Ranninger, Phys. Rev. B **70**, 104509 (2004).

27. J. Corson et al., *Nature (London)* **398**, 221 (1999).
28. Z. A. Xu et al., *Nature* **406**, 486 (2000).
29. Y. Wang et al., *Phys. Rev. Lett.* **95**, 247002 (2005).
30. O. Yuli et al., *cond-mat/0909.3963*.
31. L. P. Kadanoff and P. C. Martin, *Phys. Rev.* **124**, 670 (1961).
32. O. Tchernyshyov, *Phys. Rev. B* **56**, 3372 (1997).
33. H. Feshbach, *Ann. Phys. (N.Y.)*, **55**, 357 (1958).
34. P. W. Anderson, *Science* **235**, 1196 (1987).
35. E. Altman and A. Auerbach, *Phys. Rev. B* **65**, 104508 (2002)
36. F. Wegner, *Ann. Phys. (Leipzig)* **3**, 77 (1994).
37. J. Ranninger and A. Romano, *Phys. Rev. B* **78**, 054527 (2008).
38. T. Stauber and J. Ranninger, *Phys. Rev. Lett.* **99**, 045301 (2007).
39. J. Roehler, *Int. J. Phys. B* **19**, 255 (2005); *cond-mat/0909.1702*.
40. J. Ranninger and T. Domanski, *Phys. Rev. B* **81**, 1 (2010).
41. T. Domanski and J. Ranninger, *Phys. Rev. Lett.* **91**, 255301 (2003).
42. A. Kanigel et al., *Phys. Rev. Lett.* **101**, 137002 (2008).
43. J.-M Robin, A. Romano and J. Ranninger, *Phys. Rev. Lett.* **81**, 2755 (1998).